# Chromophore-Containing Polymers for Trace Explosive Sensors†

**Antao Chen,* Haishan Sun, Anna Pyayt, and Xunqi Zhang**

*Applied Physics Laboratory, University of Washington, Seattle, Washington 98105*

**Jingdong Luo and Alex Jen**

*Department of Materials Science and Engineering, University of Washington, Seattle, Washington 98105*

**Philip A. Sullivan, Samy Elangovan, and Larry R. Dalton**

*Department of Chemistry, University of Washington, Seattle, Washington 98105*

**Raluca Dinu, Danliang Jin, and Diyun Huang**

*Lumera Corporation, Bothell, Washington 98011*

*Received: December 17, 2007; Revised Manuscript Received: February 28, 2008*

The optical properties such as index of refraction and optical absorption of many chromophore-containing polymers are sensitive to the physical and chemical environment to which the polymers are exposed. To demonstrate such applications, chemical sensors to detect trace explosives are presented. The sensors use polymers that contain chromophores whose molecular structure consists of an electron donor and an electron acceptor connected by a charge-transfer bridge of conjugated $\pi$-orbital electrons. The polymers used for the trace explosives sensor are not poled, and the chromophores are randomly oriented in the polymer host. Waveguide microring resonator and fiber Bragg grating structures were used in these sensors to enhance the detection sensitivity. Because chromophores undergo photodecomposition under intense ultraviolet radiation, chromophore-containing polymers can be patterned with ultraviolet light to create optical resonator structures in a single photobleaching step. The chemical sensor has shown part-per-billion level sensitivity and good specificity to the vapor, in air, of an explosive simulant 2,4-dinitrotoluene.

## Introduction

Chromophores are molecules or parts of molecules that have an absorption band in the visible spectral range and give rise to color due to electron charge transfer or rearrangement and $\pi$-electron conjugation. Of various types of chromophores, those that have molecular structures of electron donor and acceptor groups connected by a conjugated bridge of $\pi$-electron orbitals (D$-\pi-$A structure) are of particular interest for our purposes. Such chromophores exhibit strong second- and third-order nonlinear optical properties, and polymers that contain such chromophores have found many applications ranging from laser harmonic generation,[1] terahertz signal generation and detection,[2] electrooptic and all-optical modulation and switching,[3–5] and optical beam scanning.[6]

In this paper we describe recent progress utilizing chromophore-containing polymers to fabricate optical sensors for trace explosives detection. By combining chromophore-containing polymers with optical resonator structures such as waveguide microring resonators and fiber Bragg gratings, a variety of sensors can be realized. Recently we have discovered that some polymers containing chromophores of D$-\pi-$A structure can have strong interaction with molecules of nitroaromatic compounds such as trinitrotoluene (TNT) and dinitrotoluene (DNT). As nitroaromatic compounds represent the major group of high explosives, this new discovery can potentially have applications in homeland security, counterterrorism, and land mine detection. Unlike electrooptic polymers,[7] poling[8] is not necessary for this application, and the chromophores are randomly oriented in the polymer matrix. This naturally avoids the thermal stability issues associated with poled nonlinear optical polymer systems. Significant changes in the UV$-$vis absorption spectra and indices of refraction have been observed when the polymer is exposed to part-per-billion (ppb) levels of DNT. A compact explosive sensor based on microresonators made in chromophore-containing polymers by photobleaching is presented. Experimental results indicate that a sensitivity level of parts per trillion can potentially be achieved.

## Change of Linear Optical Properties Caused by Nitroaromatic Compounds

Recently we have observed that the vapors of 2,4- and 2,6-dinitrotoluenes cause drastic changes in the linear optical properties, i.e., index of refraction and absorption spectrum, of certain chromophore-containing polymer thin films. Figure 1 shows the UV$-$vis$-$near-IR absorption spectra of a thin film chromophore DH6[9] (shown in Figure 2) doped in poly(methyl methacrylate) (PMMA) at 20 wt % upon exposure to DNT as a function of the duration of exposure. The polymer films were spin-coated from solution on glass slides and dried overnight in vacuum at 60$-$70 °C. The thickness of the film is 1 $\mu$m. The film is not electrically poled, and the chromophores are randomly orientated in the matrix of the PMMA host. The main absorption peak originally at 630 nm shows a red shift as large as 70 nm

† Part of the "Larry Dalton Festschrift".

* To whom correspondence should be addressed. Phone: (206) 543-1274. E-mail: antaochen@apl.washington.edu.

10.1021/jp7118372 CCC: $40.75 
Published on Web 04/29/2008

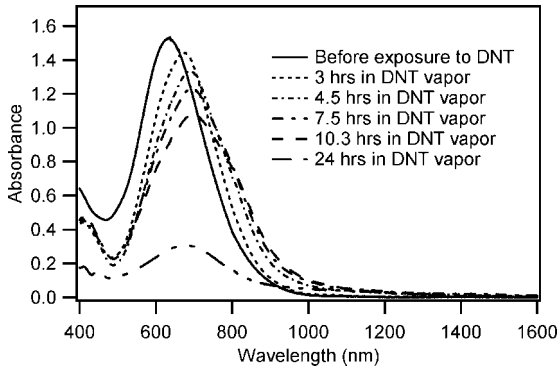


**Figure 1.** Absorption spectrum of a DH6/PMMA thin film after it is exposed to DNT vapor at 65 °C for various periods of time. The peak at about 630 nm is the characteristic absorption peak of the chromophore.

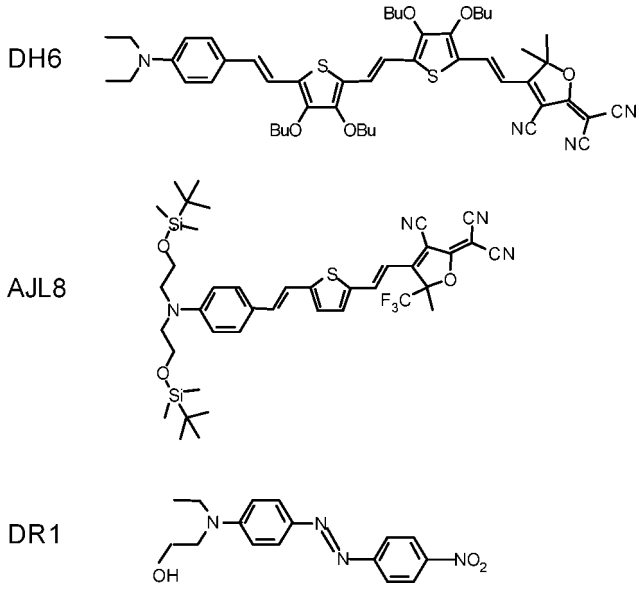


**Figure 2.** Chemical structures of the chromophores used in this study.

and a reduced peak absorbance from 1.53 to 0.3 after the film is exposed to the analyte vapor saturated in air at 65 °C for 24 h. Similar changes have also been observed at room temperature although the same degree of change took place about 10 times more slowly. The change of color of the film is also visible to the unaided eye. The color of the polymer film changes from dark blue to light purple. The changes in the absorption spectrum and the corresponding color changes were observed with a number of host polymers doped at various levels with several different chromophores (DH6,[9] AJL8,[10] and DR1[1]) of the D−$\pi$−A structure shown in Figure 2. The type of host polymer (PMMA, amorphous polycarbonate (APC), and bisphenol A-polycarbonate) and solvent (chloroform and cyclopentanone) used to make the polymer solutions have only a minor effect on the polymer thin film's response to DNT.

Accompanying the change in the absorption spectrum is a change in the index of refraction. Chromophores of D−$\pi$−A structure are highly polarizable and contribute to the index of refraction of the polymer. The polarizability, and therefore the index of refraction, can be affected by the electric field acting on the chromophore due to the local environment. The local electric field environment can, in turn, be affected by nitroaromatic explosive molecules that are highly electronegative and polar. To study the sensitivity and specificity of the polymer as

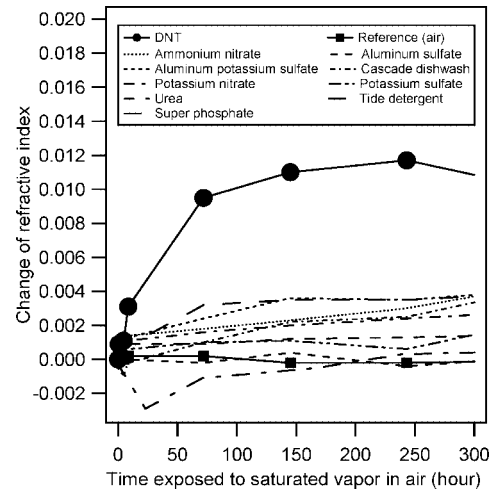


**Figure 3.** Change of the index of refraction. The change due to DNT is much larger than the change due to the other chemicals found in the environment as pollutants. The polymer is 20 wt % AJL8 chromophore in APC. The index of refraction is measured at the wavelength of 1310 nm. The lines connecting data points in Figures 3 and 5 and the fitted curves in Figures 9, 11, and 12b are only for visual guide.

trace explosive sensor materials, similarly prepared thin films of 20 wt % AJL8 chromophore in APC host were exposed to saturated vapors of DNT and to other chemicals that are a common cause of false positives of explosives sensors. These chemicals include pollutants commonly found in the environment, e.g., salts, chemical fertilizers, and detergents. The thin film samples were individually sealed in separate containers with each of these chemicals and thereby exposed to a maximum of the saturated vapor concentration of these chemicals at room temperature. The test condition represents the highest possible concentration of each of these chemicals in a natural environment, and therefore it is a meaningful indicator of sensor specificity. The concentration of saturated DNT vapor in air at room temperature is known to be 100−120 ppb.[11] The index of refraction of these thin film samples was measured at the wavelength of 1550 nm with a prism coupler (Metricon 2010) after various time periods of the exposure to the chemical vapors. Figure 3 shows the index of refraction change of these samples over time. The data show that this polymer has good specificity to DNT. The maximum refractive index change of this polymer is 0.012 at 100−120 ppb of DNT vapor concentration at room temperature. Considering that the index of refraction can be measured with a sensitivity of $10^{-7}$ with well-engineered polymer microring resonators,[12] a detection limit based on the index change of this polymer of 1 part per trillion (ppt) could be achieved. In general, the change in the index of refraction can be measured more accurately than the change in the absorption spectrum, for example, using microring resonators and fiber Bragg gratings. Therefore, sensors based on the refractive index change could be more sensitive than the sensors based on the absorption spectrum change.

The exact mechanism of how DNT molecules interact with the chromophores in the polymer matrix requires further study. Initial observations suggest, because DNT molecules are highly electron-deficient, that chromophores have an electron-rich donor and bridge and that both DNT and chromophores are highly polar; the two have a strong tendency to interact with each other. Our observation indicates that there are two processes of explosive−chromophore interaction. A relatively fast process is a red-shift of the absorption peak. The height of the absorption peak has little change. This could be due to DNT

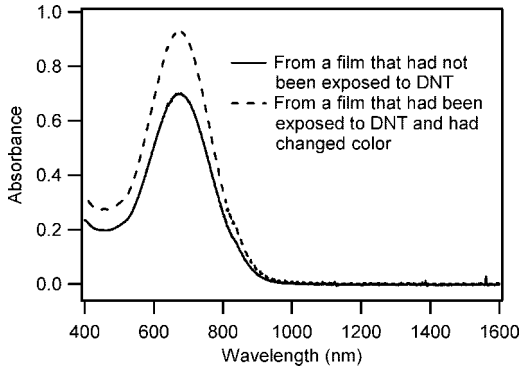


**Figure 4.** Comparison of the absorption spectra of two DH6/PMMA thin films re-dissolved in cyclopentanone. One is a pristine film without being exposed to DNT, and the other is a film that has been exposed to DNT and has changed color. After they are re-dissolved in solvent, the absorption spectra of both samples have the same peak wavelength and shape. The difference in the height of the peak is due to the difference in the concentration of the two polymer solutions.

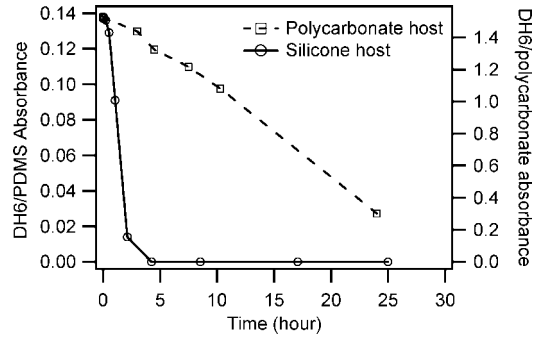


**Figure 5.** Change of peak absorbance of thin films of DH6 chromophore doped in PDMS and polycarbonate polymer hosts, respectively. PDMS is more permeable than polycarbonate and produces a more rapid response.

molecules creating a more polar environment around the chromophores, and the more polar environment leads to a solvatochromic red-shift. The time scale of this process is between several minutes to several hours, depending largely on the permeability of the host polymer. The index and absorption change of the polymer in this process is small and reversible. The second and slower process is the gradual diminishing of the absorption peak. The second process lasts a few hours (in the case of a more permeable polymer DH6 chromophore poly(dimethylsiloxane)) to a few hundred hours (in the case of a less permeable polymer AJL8 chromophore in amorphous polycarbonate). This indicates that as more DNT molecules migrate to correct sites to associate with chromophores, DNT starts to alter the band structure and disrupt the charge-transfer bands of the chromophore. The change in the absorption spectra and index of refraction in this process is large and irreversible, an evidence of the strong association between DNT and chromophore. Such interaction was only observed in solid thin films, and the spectral change does not recover even after the film is subsequently baked at temperatures above 100 °C for several days, indicating that the interaction between the chromophores and DNT is stronger than the thermal energy. Simply adding DNT to the chromophore solution does not cause any change of the chromophore absorption peak of the solution. This might be because of the overwhelming number of solvent molecules that compete against explosive molecules in interacting with chromophores. Furthermore, if the film that underwent the absorption spectrum change caused by DNT is re-dissolved in the solvent, the absorption spectrum recovers to its original shape, as shown in Figure 4. This reversibility suggests that the interaction between chromophore and DNT is physical in nature, rather than a chemical reaction. When the film is re-dissolved in the solvent, solvent molecules also interact with the chromphores and compete with DNT molecules. Since solvent molecules in the polymer solution far outnumber DNT molecules, the solvent separates the DNT molecules from the chromophores.

For the AJL8/APC polymer, saturation was not achieved until 250 h of exposure to the DNT vapor. However, the sensing polymer produces a detectable amount of refractive index change in approximately 10 min of exposure to DNT vapor of 100 ppb concentration. The response rate is thought to be limited by the diffusion of DNT molecules into the polymer. If a more permeable polymer, poly(dimethylsiloxane) (PDMS), was used as the host polymer, a 10 times improvement in the response rate was observed (Figure 5).

## Design and Fabrication of High-$Q$ Polymer Microring Resonators

In addition to sensitive sensor materials, the overall sensitivity of a sensor can also be greatly enhanced by incorporating optical resonator structures (such as microresonators and fiber Bragg gratings) in the sensor design. In these resonators, light at the resonant wavelength makes a large number of passes through the sensor material in the resonator cavity, and therefore the effect of the sensor material on the optical wave is significantly amplified. Microring resonators show great promise for sensor applications because of their sharp resonances and compact size. A wide range of optical signal processing functions, including channel filters, wavelength division multiplexers, switches, dispersion compensators, lasers, polarization rotators, and modulators, can be realized with microring resonators.[13] The resonant properties of microring resonators also makes them an ideal platform for optical sensors.[12] The small device size makes it possible to integrate a large number of sensors of different functions on the same chip and also requires a smaller amount of analyte for biological and chemical sensing.

Basic microring resonators consist of a simple ring waveguide as a resonant cavity and one or two straight bus waveguides that couple to the ring waveguide and provide input and output ports. When the round-trip phase shift over the ring waveguide is equal to multiples of $2\pi$, circulating photons interfere constructively with each other and build up the resonant energy in the ring. At resonance, light from the input port is totally trapped and dissipated in the ring cavity, and a resonance notch in the transmitted energy occurs at the through port output (Figure 6a,b). If there is a second bus waveguide coupled to the ring, the light trapped in the ring will be coupled out to the second bus waveguide, and a resonance peak will be produced at the drop port (Figure 6c,d). Because the phase shift $\theta = 2\pi n_{\text{eff}} L/\lambda$, where $n_{\text{eff}}$ is the effective refractive index of the ring waveguide, $L$ the circumference of the ring, and $\lambda$ the free-space wavelength of the light, the resonant wavelength is a function of $n_{\text{eff}}$. When $n_{\text{eff}}$ is varied by an applied electric field or by the electric fields associated with analytes, a shift of resonant wavelengths occurs.

The $Q$ factor is the most important figure-of-merit of resonators. $Q$ is defined as the ratio of resonant wavelength to the full width at half-maximum of the resonance line width. Higher $Q$ leads to sharper slopes of resonances and sensors of higher sensitivity. High-$Q$ microring resonators can be achieved

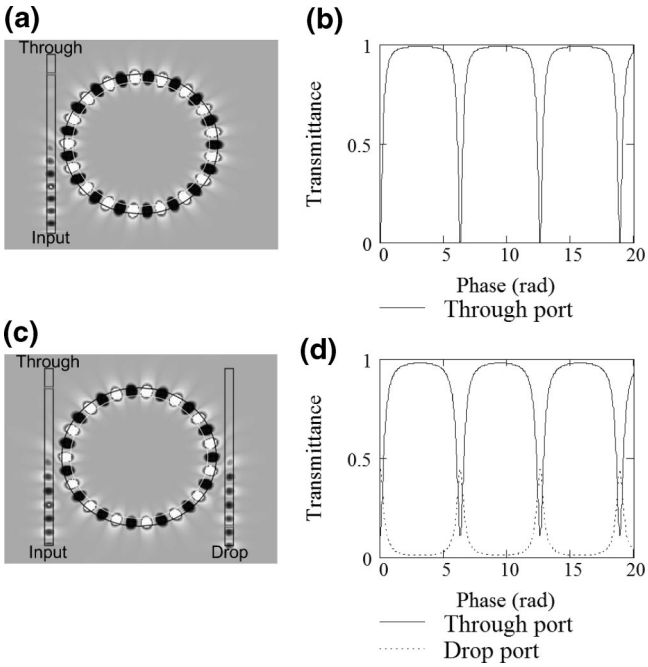


**Figure 6.** Basic microring resonator structures: (a) one ring resonator and one bus waveguide and (b) the corresponding resonance spectrum at the through port; (c) one ring resonator and two bus waveguides and (d) the corresponding resonance spectra at the through port and the drop port.

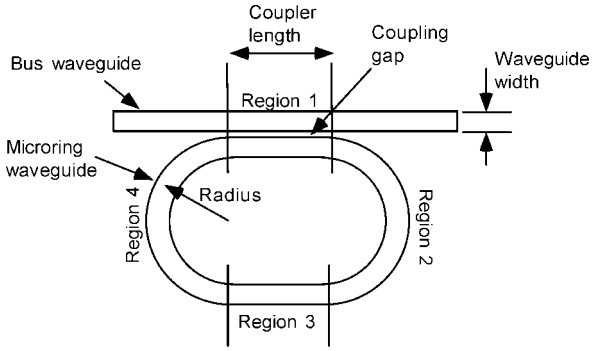


**Figure 7.** Basic microring resonator. By considering a basic microring resonator as an optical system composed of a directional couplers (region 1) and curved waveguides (regions 2−4 combined), effects of device parameters can be separated to simplify the computer modeling.

through systematic design and optimization with numerical simulations. The finite difference time domain (FDTD) method gives a full solution of Maxwell's equations and does not involve any approximations or theoretical restrictions, and it is the rigorous method to simulate microring resonator devices. However, the FDTD algorithm is very computation-intensive, slow, and requires a very large amount of computer memory. Cluster computers, not available to most of scientific researchers, are normally required to run FDTD codes.

We developed a simple approach to design microring resonators. Our approach is far less computationally intensive yet still effective. The microring resonators are considered as an optical system composed of directional couplers and waveguide bends that provide feedback from the output of the coupler to its input (Figure 7). Directional couplers and waveguide bends can be satisfactorily modeled with transfer matrices.[14,15] The elements of the transfer matrices can be calculated with good accuracy using a beam propagation method (BPM) code, which uses a simplified algorithm and assumes several approximations.

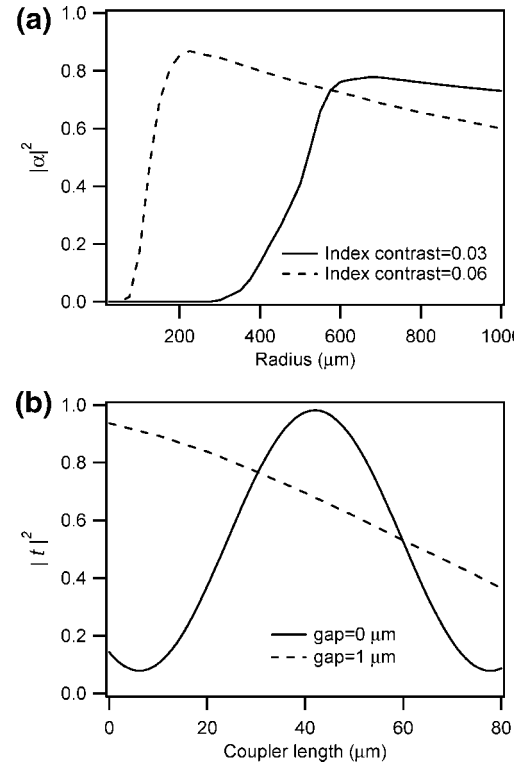


**Figure 8.** Simulation results for polymer microring resonators: (a) Round trip attenuation as a function of radius of curvature for two index contrast cases; (b) coupling-induced attenuation as a function of coupler length for two gap width cases. The wavelength of the simulation is 1.55 $\mu$m. Both the thickness of the polymer film and the width of the waveguide are 2 $\mu$m, and the index of refraction of the polymer waveguide core is 1.65.

However, the computation is much faster than a FDTD code. BPM is not capable of handling the microring resonator device as a whole but can accurately model the directional couplers and waveguide bends, the two building blocks of the resonator. Combinations of the transfer matrices will produce transmission characteristics for every output port. Using the laterally coupled microring resonator as an example, we investigated the effects of waveguide width, ring radius, refractive index contrast, and coupling length and gap, on the internal loss factor $\alpha$[14] and coupling loss factor $t$[14] with BPM simulations.

Typically, the widths of ring resonators only support a single transverse mode (of a particular polarization). Inside the single mode range, wider waveguides can confine the light more tightly in the waveguide, thus decreasing both scattering loss and radiation loss and giving a larger $\alpha$. With a certain waveguide surface roughness and material absorption loss, both an optimal ring radius and refractive index contrast exists, and a higher index difference normally requires a smaller optimal radius (Figure 8a). The simulation shows that if the index contrast is equal or smaller than 0.03, the radius should be at least 500 $\mu$m to avoid excessive round trip attenuation. If the index contrast is bigger than 0.06, a high-$Q$ microring resonator with radius as small as 200 $\mu$m is possible. For any desired $t$, a series of best combinations of the coupling length and coupling gap size can be selected from the simulations (Figure 8b). The design procedure is to find an appropriate bend radius for the index contrast of the waveguide in order to maximize $\alpha$ using data similar to those plotted in Figure 8a, and then use data similar to those plotted in Figure 8b to find the best coupler length and gap to match $t$ with $\alpha$. This will lead to the highest $Q$ and

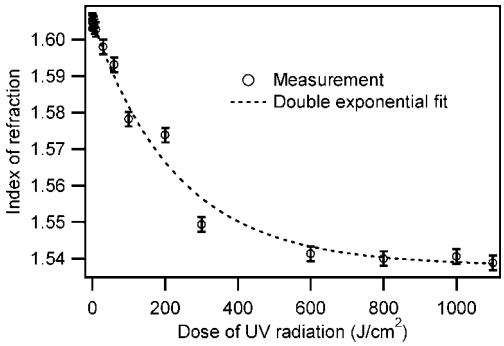


**Figure 9.** Change in the refractive index of AJL8/APC film after the film is photobleached at various doses.

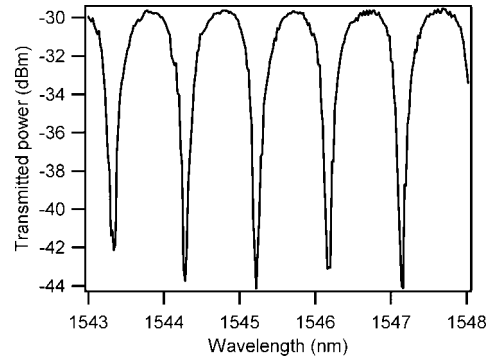


**Figure 10.** Measured transmission spectrum of a microring resonator made in AL8/APC by photobleaching. The width of the waveguide is 4 $\mu$m. The coupling gap is 1.1 $\mu$m, and the length of the coupling region is 80 $\mu$m.

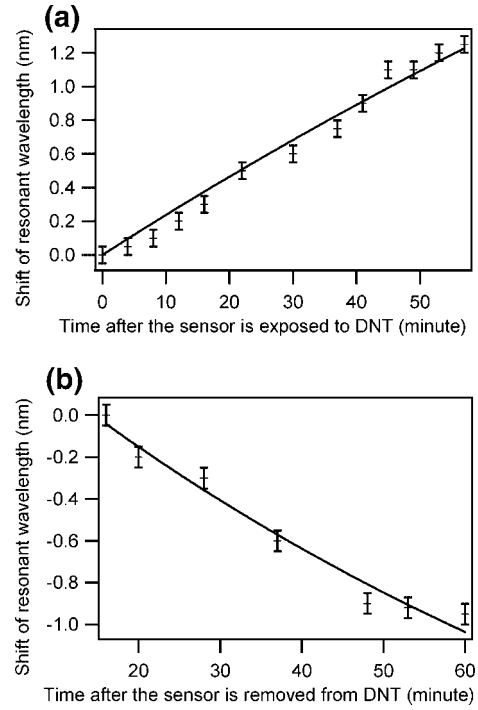


**Figure 11.** Otput of the sensor when it is exposed to (a) and removed from (b) saturated DNT vapor at room temperature.

extinction ratio. Wider gap (>1 $\mu$m) or zero gap designs are easiest to fabricate and are preferable.

The use of polymer materials offers a number of advantages for making microring resonator devices. With the same waveguide surface roughness, low refractive index contrast between the polymer waveguide core and cladding (which contributes to the main loss mechanism and compromises the *Q*-factor of microring resonators), leads to lower scattering loss. Low refractive index and large cross-section (for single mode guiding) of the polymer waveguide provide better coupling efficiency to optical fibers, which can significantly reduce the device insertion loss. Device fabrication processes that do not work with other materials may be applicable to polymers. A unique property of chromophore-containing polymers is that optical waveguides and resonators can be fabricated in these polymers through a simple, one-step, dry process termed photobleaching. During photobleaching high-energy photons of UV wavelengths decompose the conjugated-electron system of the organic chromophores. This decomposition bleaches out the color of chromophores and reduces the polarizability and the index of refraction of the chromophore-containing optical polymer. Photobleaching has been used to make channel waveguides[16,17] and to perform postfabrication trimming[18] of polymer waveguide devices. Photobleaching is a single-step process, which not only simplifies the device fabrication but also reduces the sources of error from multiple fabrication steps. Photobleaching also does not involve wet chemistry which may not be compatible with chromophore-containing polymers.

The polymer used in this study was amorphous polycarbonate (APC) doped with 25 wt % of AJL8 chromophore.[10] Figure 9 gives the refractive index change after various doses of photobleaching, indicating a permanent and stable change in the material. The refractive index was measured at the wavelength of 1550 nm, and the photobleaching was carried out using a mercury discharge lamp with emission peaks at 365 and 402 nm. The photobleached film loses its dark blue color and becomes completely clear and colorless. It also loses the sensitivity to DNT vapor. An index of refraction decrease of as much as 0.066 is observed after the color of the polymer film is completely bleached out.

Photobleaching also reduces the thickness of the EO polymer by a few percent. This is because some of the photodecomposition products are gaseous and leave the polymer thin film, reducing the volume of the solid polymer. The photobleached region has the same level of surface smoothness as the unbleached region. Waveguide losses were measured by the cutback method.[19] The propagation loss was found to be 2.3 and 2.0 dB/cm for the transelectric (TE) and transmagnetic (TM) polarizations, respectively. These are similar to the losses of the ridge waveguides made from the same material by photolithography and reactive ion etching (RIE), which are conventional methods to make waveguides in polymer thin films. Coupling loss from the fiber to the waveguide was 4 dB for each coupling interface, which is a typical value for the polymer waveguides with the same mode size.

On the basis of these measurement and simulation results, race-track-shaped microring resonators were designed with 4 $\mu$m wide waveguide, 80 $\mu$m coupling length, and 200 $\mu$m radius. Samples with coupling gaps ranging from 0.6 to 1.2 $\mu$m were tested. It was found that resonators with a coupling gap of 1.1 $\mu$m had the highest extinction ratio. Extinction ratios larger than 10 dB can be routinely obtained (Figure 10). The free spectral range between adjacent resonances was approximately 1.08 nm, which is in good agreement with the theoretical calculation. The *Q* factor of the resonators obtained from curve fitting is in the range of 6500−8100 and is adequate for sensor applications. The insertion loss at the peak transmission was 8.7 dB, mainly attributed to the fiber−waveguide coupling.

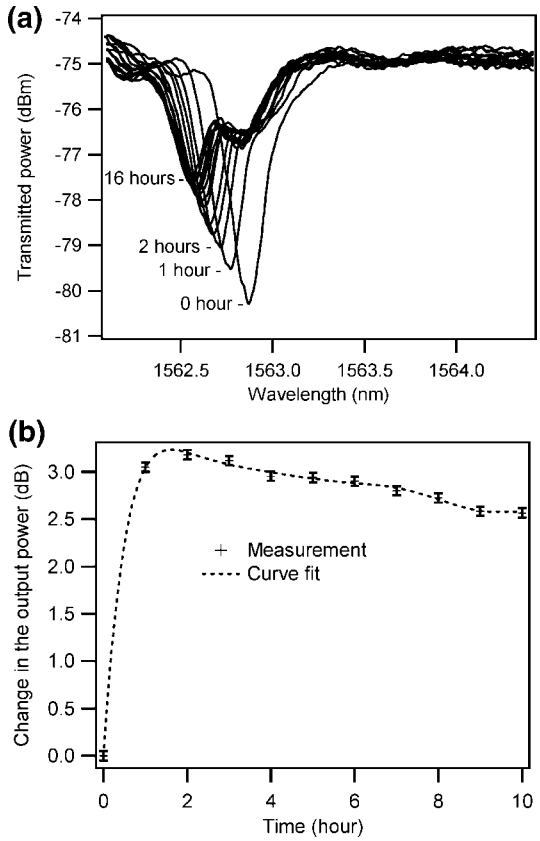


**Figure 12.** (a) Change in the transmission spectrum of a fiber Bragg grating coated with DH6/PMMA in response to DNT. The sensor was exposed to saturated DNT vapor at room temperature. The measurements were taken at time intervals of 1 h. The last measurement was taken after the sensor was exposed to DNT for 16 h. (b) The change of optical power at the output end of the fiber sensor for light of the wavelength of 1562.9 nm.

### Chemical Sensor for Trace Explosive Detection

The microring resonators of the 25 wt % AJL8/APC polymer fabricated with photobleaching were exposed to the saturated DNT vapor at room temperature. A resonance shift toward longer wavelength was observed (Figure 11a), indicating an increase in the refractive index of the polymer consistent with the thin-film refractive index measurement results. This response originates from the change of the index of refraction of the core of the channel waveguide, which was shielded by the metallic pattern of the photomask and not photobleached. After 1 h of exposure, the shift was 1.2 nm and the maximum effect has not yet been reached. After removing the sensor from the DNT atmosphere, the sensor properties returned to their initial conditions (Figure 11b). Our current test setup can measure the resonant wavelength to an accuracy of 0.05 nm. This accuracy corresponds to an accuracy of 0.00005 for index of refraction measurements, and a sensitivity of $\sim$5 ppb. Sensitivity at this level is comparable to explosive sensors based on fluorescence quenching, which are also typically tested at parts per billion levels. Unlike sensors based on fluorescence quenching and lasing action, the sensors of this work do not require the use of short wavelength excitation which can photobleach the sensor materials. Polymer microring resonators with optimized design and fabrication conditions have demonstrated an index of refraction measurement accuracy of $10^{-7}$, which corresponds to a detection sensitivity of a few parts per trillion.

In addition to polymer waveguide microring resonators, we also made trace explosives sensors by incorporating a fiber Bragg grating with the same polymer. The grating section of the fiber is first etched with hydrofluoric acid and the diameter of the fiber is reduced from 125 to about 30 $\mu$m. This allows the evanescent tail of the fiber mode to extend into the polymer coating to probe the change of the refractive index of the polymer. The polymer is coated on the etched area of the fiber by dipping the fiber in the polymer solution and letting the coating dry with the fiber held in a vertical position. The thickness of the coating is about 1 $\mu$m. The change in the index of refraction of the polymer coating shifts the resonance of the fiber and changes the output optical power at a wavelength fixed at the maximum slope of the resonance, as shown in Figure 12. After the sensor fiber is exposed to saturated DNT vapor in air at room temperature for over 16 h, the change in the properties of the polymer become so large that not only is the resonance wavelength shifted but the shape of the resonance is also greatly altered and distorted. Since both microring resonators and fiber Bragg gratings are high-$Q$ optical resonators, the microring resonators sensors and fiber Bragg grating sensors should have comparable sensitivity and response rate if the sensor film of the same polymer and same thickness is used.

### Conclusions

In addition to the more traditional applications of poled electrooptic polymers and unpoled chromophore-containing polymers also have potential applications in chemical and environmental sensors. Novel trace explosives sensors using chromophore-containing polymer are successfully demonstrated. High-$Q$ factor of polymer microring resonators can be achieved through systematic design and optimization with fast BPM simulations and transfer matrix analysis. A photobleaching technique is capable of fabricating high-quality microring resonators in chromphore-containing polymers. It is a single-step process that does not involve wet chemistry or toxic gases. Microring resonators made with chromophore-containing polymer can be used to detect trace explosives. Detection sensitivity of DNT at part per billion level with good specificity has been demonstrated, and the polymer has the potential of pushing the detection limit at the part per trillion level.

**Acknowledgment.** This work is supported by National Science Foundation (NSF) Grant No. ECS-0437920, an NSF Center on Materials and Devices for Information Technology Research (CMDITR) Grant No. DMR-0120967, and an ONR Grant N00014-05-1-0843.

### References and Notes

(1) Samoc, A.; Samoc, M.; Luther-Davies, B.; Kolev, V. Z.; Bagien, R. K.; Luo, X.; Zha, C. *Mol. Cryst. Liq. Cryst.* **2006**, *446*, 123.

(2) Zheng, X.; Sinyukov, A.; Hayden, L. M. *Appl. Phys. Lett.* **2005**, *87*, 81115.

(3) Lee, M.; Katz, H. E.; Erben, C.; Gill, D. M.; Gopalan, P.; Heber, J. D.; McGee, D. J. *Science* **2002**, *298*, 1401.

(4) Shi, Y.; Zhang, C.; Zhang, H.; Bechtel, J. H.; Dalton, L. R.; Robinson, B. H.; Steier, W. H. *Science* **2000**, *288*, 119.

(5) Hochberg, M.; Baehr-Jones, T.; Wang, G.; Shearn, M.; Harvard, K.; Luo, J.; Chen, B.; Shi, Z.; Lawson, R.; Sullivan, P.; Jen, A. K. Y.; Dalton, L.; Scherer, A. *Nat. Mater.* **2006**, *5*, 703.

(6) Maki, J. J.; Cao, G.; Taboada, J. M.; Tang, H.; Tang, S.; Chen, R. T. *Proc. SPIE* **1998**, *3281*, 55.

(7) Steier, W. H.; Kalluri, S.; Chen, A.; Garner, S.; Chuyanov, V.; Ziari, M.; Shi, Y.; Fetterman, H.; Jalali, B.; Wang, W.; Chen, D.; Dalton, L. R. *Electr., Opt., Magn. Prop. Org. Solid State Mater. III, Symp.* **1996**, 147.

(8) Herminghaus, S.; Smith, B. A.; Swalen, J. D. J. *Opt. Soc. Am. B* **1991**, *8*, 2311.

(9) Jin, D.; Londergan, T.; Huang, D.; Wolf, N.; Condon, S.; Tolstedt, D.; Guan, H. W.; Cong, S.; Johnson, E.; Dinu, R. *Proc. SPIE* **2004**, *5351*, 44.

(10) Luo, J.; Liu, S.; Hailer, M.; Kang, J.-W.; Kim, T.-D.; Jang, S.-H.; Chen, B.; Tucker, N.; Li, H.; Tang, H.-Z.; Dalton, L. R.; Liao, Y.; Robinson, B. H.; Jen, A. K. Y. *Proc. SPIE* **2004**, *5351*, 36.

(11) Jose, A.; Zhu, Z.; Madigan, C. F.; Swager, T. M.; Bulovic, V. *Nature* **2005**, *434*, 876.

(12) Chao, Ch.-Y.; Fung, W.; Guo, L. J. *IEEE J. Sel. Top. Quantum Electr.* **2006**, *12*, 134.

(13) Little, B. E.; Chu, S. T. *Opt. Photonics News* **2000**, 24.

(14) Yariv, A. *Electron. Lett.* **2000**, *36*, 321.

(15) Paloczi, G. T.; Huang, Y.; Yariv, A.; Mookherjea, S. *Opt. Express* **2003**, *11*, 2666.

(16) Ma, J.; Lin, S.; Feng, W.; Feuerstein, R. J.; Hooker, B.; Mickelson, A. R. *Appl. Opt.* **1995**, *34*, 5352.

(17) Zhou, J.; Pyayt, A.; Dalton, L. R.; Luo, J.; Jen, A. K. Y.; Chen, A. *IEEE Photonics Technol. Lett.* **2006**, *21*, 2221.

(18) Chen, A.; Chuyanov, V.; Marti-Carrera, F. I.; Garner, S.; Steier, W. H.; Mao, S. S. H.; Ra, Y.; Dalton, L. R.; Shi, Y. *IEEE Photonics Technol. Lett.* **1997**, *9*, 1499.

(19) Nordstrom, M.; Zauner, D. A.; Boisen, A.; Hubner, J. J. *Lightwave Technol.* **2007**, *25*, 1284.

JP7118372